

## The simulation of a laminar flow in a local constriction of a pipe by a cellular automaton\*

Yu.G. Medvedev

**Abstract.** A two-dimensional case of the process of laminar flow passing through a pipe constriction is investigated. The two-dimensional statement corresponds to the case with a three-dimensional flow between two parallel planes. A cellular automaton model of a flow is used, which has an integer alphabet of cell states and a synchronous operation mode. The dependences of the velocity and pressure on the coordinate along the direction of a flow for different constriction clearances and different pressure gradients at the ends of the pipe are obtained.

### Introduction

At present, the possibility of applying discrete methods of simulation [1] to problems of spatial dynamics [2] is being actively studied, since these methods make it possible to obtain relatively simple software implementations on modern supercomputers [3]. One of the discrete models — the cellular automaton model of the gas flow FHP-MP [4] is used in this study.

The objective of this paper is to check the possibility of using the model under study in conditions of a flow in a straight pipe at a constant temperature in a subcritical mode; under these conditions, the critical Reynolds number makes up several thousands[5].

This paper investigates a gas flow passing in the space between parallel flat walls (Figure 1a).

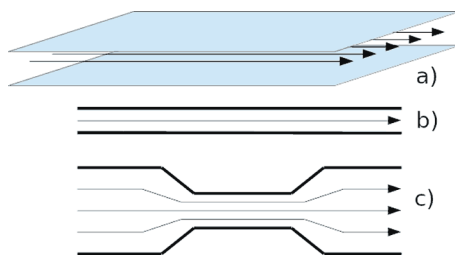


**Figure 1.** A flow diagram between parallel planes: a) without constriction in the three-dimensional form; b) without constriction in the two-dimensional form; c) with constriction in the two-dimensional form

This flow corresponds to the two-dimensional case shown in Figure 1b, and is described in [5, §17]. Since the characteristics of the three-dimensional flow between two parallel planes and in a pipe with a circular cross-section,

---

\*Supported by the State Contract with ICMMG SB RAS (251-2021-0005). Simulations have been performed on the cluster of JSCC RAS.

not considered here, differ only in coefficients, for brevity we will call the described two-dimensional structure a pipe. So, the constriction or a variable distance between the planes in the three-dimensional case corresponds to the variable diameter of the two-dimensional pipe (Figure 1c).

The sought for dependencies are the distribution of velocity and pressure along the direction of a flow for different constriction clearance and different pressure gradients at the ends of the pipe.

We pose the problem of simulating a flow with the boundary conditions just described using the FHP-MP discrete cellular automaton model and comparing it with the known results obtained using continuous methods. Such a comparison is needed as part of the investigation into the feasibility of using the discrete model.

## 1. Description of the model

The two-dimensional simulating area is covered with hexagonal cells  $c_0, c_1, \dots, c_6, \dots$  arranged in a regular structure, each one having six neighbors (Figure 2).

Each cell is assigned to one of the three types, and it performs a simple transition function, depending on its type:

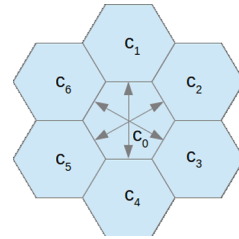


Figure 2

- conventional— the flow spreads through such cells;
- wall— the boundaries of the pipe and obstacles are built from such cells;
- valve— gas enters or exits the pipe through such cells.

The state of a cell  $c_0$  is a vector of six integers, those denote the number of discrete model particles with the unit mass and the unit velocity directed towards one of the six neighboring cells  $c_1, \dots, c_6$ . In Figure 2, these directions for the cell  $c_0$  are shown by arrows.

The cellular automaton operates in a synchronous mode [6] using an iterative transition function. The iteration has two steps: collision and propagation.

Upon collision, the velocity vectors of particles in each cell are changed, regardless of the states of the other cells:

- conventional cell— a new state is equiprobably selected from all possible states that preserve the total mass and total momentum of particles in the cell;
- wall— in a new state, the velocity vector of each particle is replaced by a counter-directional one;

- valve—in a new state, a predetermined number of particles is installed into the cell, called the nominal concentration of this valve.

Upon propagation, each particle from the cell  $c_0$  moves to one of the neighboring cells  $c_1, \dots, c_6$  in the direction of its velocity vector. Particles from the neighboring cells with oppositely directed velocity vectors, in turn, move into the cell  $c_0$ , while no particles interact with each other.

The simulation result is a velocity field and a pressure field obtained after the required number of iterations in the following way. In Figure 3, the points at which the value of the velocity and the pressure are calculated are indicated; those ones form the corresponding fields. An averaging neighborhood at each such point is a set of cells whose centers are located at a distance from this point no further than a certain averaging radius.

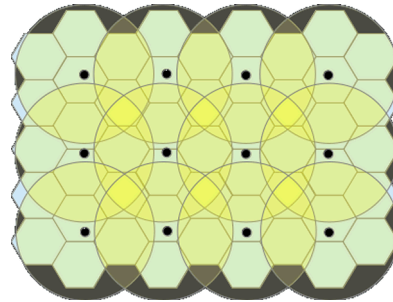


**Figure 3.** Averaging vicinities

The vicinities are indicated in Figure 3 by circles. Depending on the step and size, the averaging vicinities can intersect or be at some distance from each other.

The flow velocity at a point is the average velocity of particles located in the cells of the averaging neighborhood. The average velocity, in contrast to the velocity of the model particles, can be directed not only towards one of the neighboring cells, and its modulus does not have to be equal to unity. The gas pressure at a point is proportional to the concentration of the particles located in the cells belonging to the averaging neighborhood centered at this point.

Since the velocity of particles has a discrete direction and modulus, and the mass of particles is unity, the resulting averaged values of velocity and concentration will have some inaccuracy, called the discrete model noise.

The larger is the averaging radius, the more discrete particles are involved in calculating each value of the averaged velocity and concentration. Consequently, the less the discrete noise of the model is expressed; but at the same time the high-frequency component of the flow characteristics is roughened up, i.e. small vortices, pressure drops, etc. vanish.

In addition, if cells of obstacles or valves fall into the vicinity of the averaging, then the averaged value may be calculated incorrectly; since particles from cells located on different sides of this obstacle can be involved, where, possibly, the flow moves in other direction. Therefore, in this case, we assume the averaged values of velocity and concentration to be undefined. This condition does not allow calculating the velocity and pressure fields at a distance less than the averaging radius from obstacles.

## 2. Computer simulations

The simulating process takes place at three stages [7]:

1. Setting initial conditions.
2. Launching the simulator.
3. Averaging and visualization of the result.

These steps for the case under study are described below.

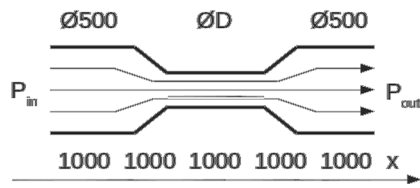


**Figure 4.** Computer simulation scheme

**2.1. Initial conditions.** Figure 4 schematically shows the cellular array, on which the pipe walls are marked. Dimensions of the cellular array are given in relative model length units, which are equal to the distance between the centers of the neighboring cells:

- pipe length — 5000 cells;
- 0000–1000 cells — wide part;
- 1000–2000 cells — constriction;
- 2000–3000 cells — constricted part;
- 3000–4000 cells — expansion;
- 4000–5000 cells — wide part;
- diameter of the wide part is 500 cells;
- diameter of the constricted part  $D = 100, 200, 300,$  or  $400$  cells (for four simulations).

As before, a pipe means a 2D structure that describes an analogue of a 3D flow between two parallel planes. Accordingly, the distance between the planes in this section of this pipe will be called the diameter.

The walls were defined as two polylines with vertices in the following coordinates for each of the four simulations.

**Simulation 1.** Clearance of the constricted part  $D = 100$  cells.

1st:  $(0, 0), (1000, 0), (2000, 200), (3000, 200), (4000, 0), (5000, 0)$ .

2nd:  $(0, 500), (1000, 500), (2000, 300), (3000, 300), (4000, 500), (5000, 500)$ .

**Simulation 2.** Clearance of the constricted part  $D = 200$  cells.

1st:  $(0, 0), (1000, 0), (2000, 150), (3000, 150), (4000, 0), (5000, 0)$ .

2nd:  $(0, 500), (1000, 500), (2000, 350), (3000, 350), (4000, 500), (5000, 500)$ .

**Simulation 3.** Clearance of the constricted part  $D = 300$  cells.

1st: (0, 0), (1000, 0), (2000, 200), (3000, 200), (4000, 0), (5000, 0).

2nd: (0, 500), (1000, 500), (2000, 400), (3000, 400), (4000, 500), (5000, 500).

**Simulation 4.** Clearance of the constricted part  $D = 400$  cells.

1st: (0, 0), (1000, 0), (2000, 50), (3000, 50), (4000, 0), (5000, 0).

2nd: (0, 500), (1000, 500), (2000, 450), (3000, 450), (4000, 500), (5000, 500).

In all simulations, the inlet valve is located on the segment with coordinates (0, 0) – (0, 500), the outlet valve is located on the segment with coordinates (5000, 0) – (5000, 500).

**2.2. Simulation parameters.** To establish a stationary flow mode, 100K iterations were performed in each simulation.

The nominal concentration of the inlet valve was set to 60 particles per cell, and the nominal concentration of the outlet valve was 20 particles per cell. Due to the peculiarities of the software implementation of the valve function, the observed averaged concentration of particles near the inlet and outlet valves does not coincide with the nominal concentration of the valves and is given in the table below.

The sought for dependencies are the distribution of velocity and pressure along the direction of flow for different constriction clearance and different pressure gradients at the ends of the pipe.

To calculate the averaged particle concentration, the averaging radius was chosen to be equal to five cells. To calculate the average particle velocity, the averaging radius was chosen equal to twenty cells.

**2.3. Averaging and visualization of the result.** Computer-aided simulation was carried out with a cellular array of 5000 by 500 cells. The pipe constriction clearance varied from 100 to 400 cells. The velocity field and the pressure field of the investigated flow are shown in Figure 5. The length

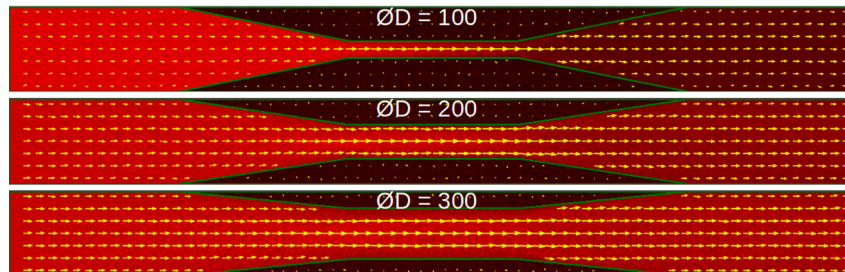


**Figure 5.** The velocity field and the pressure field of the flow obtained as a result of computer simulation for different diameters of the constricted part of the pipe

and direction of each vector shown in the figure are proportional to the magnitude and direction of the flow velocity at the corresponding point.

Background brightness is proportional to pressure: the darker areas correspond to the lower gas pressure. The figure shows that for each simulation the left part of the pipe is lighter than the right one, i.e. the pressure in it is higher, which corresponds to the physical view of the process. This effect predictably appears to be greater for those simulations in which the pipe is more constricted.

### 3. Discussion of the results

The computer simulation was carried out with a cellular array of  $5000 \times 500$  cells. The pipe constriction clearance varied from 100 to 400 cells. The velocity field and the pressure field of the investigated flow are shown in Figure 5. The length and direction of each vector shown in the figure are proportional to the magnitude and direction of the flow velocity at the corresponding point.

Background brightness is proportional to pressure: the darker areas correspond to the lower gas pressure. The figure shows that for each simulation the left part of the pipe is lighter than the right one, i.e. the pressure in it is higher, which corresponds to the physical view of the process. This effect predictably appears to be greater for those simulations in which the pipe is more constricted.

Figure 6 shows an enlarged rectangular fragment of the cellular array used in simulation 1 with the upper left and the lower right corners coordinates equal to  $(3500, 350)$  and  $(3750, 450)$ , respectively, in which a more detailed averaging of the velocity and concentration of particles was per-

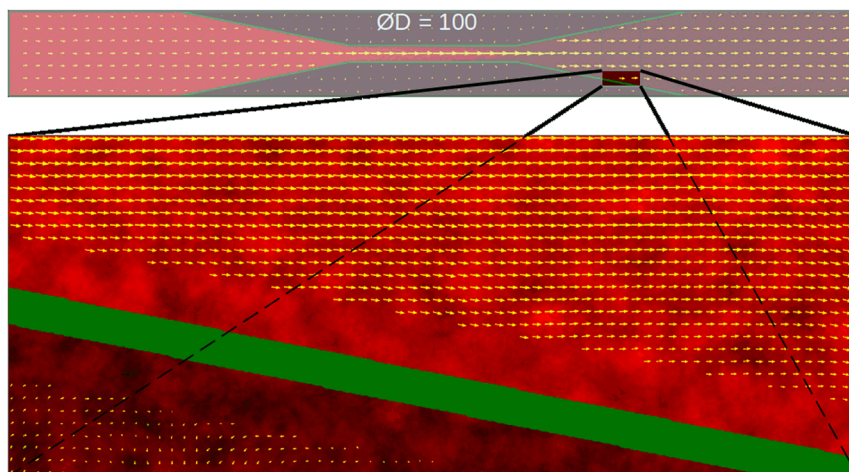


**Figure 6.** A fragment of the velocity and pressure fields

formed. It can be seen from the figure that the flow turned to be laminar: no vortices are formed in it; in the expanding section of the pipe, the gas moves uniformly even near the wall.

As is mentioned above, the correct values of the averaged velocity and pressure cannot be obtained at a distance less than the averaging radius from obstacles (5 cells for pressure and 20 cells for velocity in our case); thus, a wall with a thickness equal to one cell is depicted with two additional averaging radii over its thickness (11 cells, 5 additional cells in each direction), and the boundary of the velocity field is 20 cells from the wall (or 15 cells from the boundary of the wall image).

The table shows relationship between the constriction clearance and the gas pressure gradient  $dp = P_{\text{in}} - P_{\text{out}}$  at the ends of the pipe, where  $P_{\text{in}}$  and  $P_{\text{out}}$  are the pressure at the inlet and the outlet of the pipe, respectively (see Figure 4). These pressures depend on many factors – valve nominal pressure, flow velocity and other characteristics. The experimentally obtained normalization coefficient  $k$  is also indicated for the flow velocity; it equalizes the wide section velocity for all the four simulations  $k_1 v_1 = k_2 v_2 = k_3 v_3 = k_4 v_4 = 1$ , where  $k_i$  and  $v_i$  are the normalization coefficient and the velocity in a wide section of the pipe in the  $i$ th simulation. The velocity is given in relative model units, the coefficient  $k$  is dimensionless.

$D$	$dp$	$k$
100	23.8	0.28
200	9.8	0.14
300	3.7	0.11
400	1.9	0.10

The distribution of the longitudinal component of the flow velocity along the pipe, averaged over the cross-section, obtained in each of the four simulations, is shown in Figure 7. It can be seen from the figure that, using the normalization coefficients, it was possible to combine the lower parts of the graphs, corresponding to the velocities in wide sections at the beginning

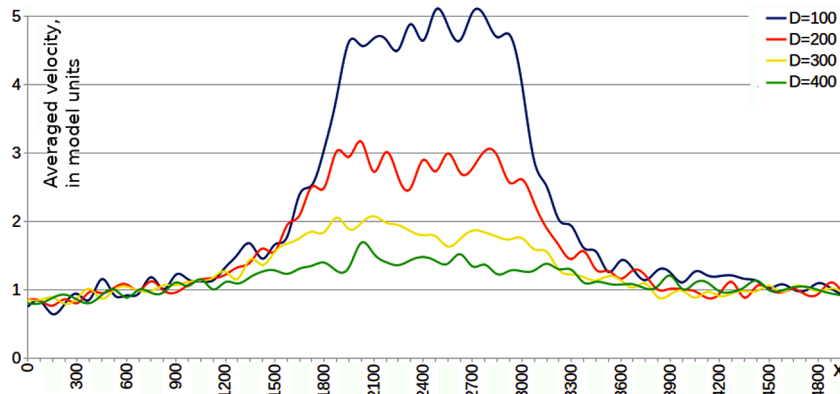


**Figure 7.** Velocity distribution along the direction of flow for different constriction clearance

and at the end of the pipe. In the middle of the pipe, in its constricted part, the flow velocity is maximum in each of the simulations. A comparison of the simulations also shows that this velocity has an inverse dependence with the diameter of the constricted part of the pipe, which corresponds to the existing concepts of the physics of the process.

### Conclusion

The velocity and pressure fields of the gas in a two-dimensional pipe are obtained. Velocity and pressure distributions along the flow direction are constructed for different constriction clearances and different pressure gradients at the ends of the pipe. The possibility of using the investigated model under conditions of flow spreading in a straight pipe at a constant temperature in a subcritical mode with a critical Reynolds number about several thousands is shown. The simulation results are consistent with the known data. This allows us to conclude that the FHP-MP cellular automaton gas flow model adequately simulates the laminar flow in a pipe.

### References

- [1] Schiff J.L. Cellular Automata: A Discrete View of the World. — New Jersey: John Wiley & Sons Inc., 2008.
- [2] Chopard B. Cellular Automata Modeling of Physical Systems // Computational Complexity / R. Meyer ed. — New York: Springer, 2012. — P. 407–433.
- [3] Bandman O. Cellular automata diffusion models for multicomputer implementation // Bull. Novosibirsk. Comp. Center. Ser. Computer Science. — Novosibirsk, 2014. — Iss. 36. — P. 21–31.
- [4] Medvedev Yu. The FHP-MP model as multiparticle Lattice-Gas // Bull. Novosibirsk. Comp. Center. Ser. Computer Science. — Novosibirsk, 2008. — Iss. 27. — P. 83–91.
- [5] Landau L.D., Lifshits E.M. Theoretical Physics. Vol. VI. Hydrodynamics. — 5th ed. — Moscow: Fizmatlit, 2001 (In Russian).
- [6] Bandman O. Parallel composition of asynchronous cellular automata simulating reaction diffusion processes // Proc. 9th Intern. Conf. on Cellular Automata, (ACRI-2010). — Springer, 2010. — P.395–398. — (Lect. Notes in Comp. Sci.; 6350).
- [7] Gorodnichev M., Medvedev Yu. A web-based platform for interactive parameter study of large-scale lattice gas automata // PaCT-2019 Proc. — Springer, 2019. — P. 321–333. — (Lect. Notes in Comp. Sci.; 11657).